GEOPHYSICAL RESEARCH LETTERS, VOL. 27, NO. 24, PAGES 4021-4024, DECEMBER 15, 2000

Polar Cap X-rays and Electrons under Low Density Solar Wind Conditions: Coordinated PIXIE and DMSP Observations on 11 May 1999

P. C. Anderson,[1] D. L. McKenzie,[1] D. W. Datlowe,[2] J. D. Hawley,[2] S. M. Petrinec,[2] M. Schulz,[2] and D. E. Larson[3]

Abstract. X-ray images from 11 May 1999 typically show emissions filling a region above about 75° – 80° magnetic latitude with the emitting region centered a few degrees toward mid-morning from the magnetic pole during a period when the solar wind reached unusually low values. Ionospheric particle measurements show the entire northern polar cap illuminated by precipitating electrons during much of this time, while the southern polar cap was mostly "dark." The precipitating electrons had multicomponent spectra, one component with characteristic energy ~200 eV throughout the observation period, and others with time-varying characteristic energies ranging between ~3.5 keV and 10 keV, all components with spatial characteristics common to polar rain. Measurements in the solar wind also show similar multicomponent spectra and are relatively well correlated with observations of solar radio bursts and the polar-cap x-ray flux. We conclude that the higher energy components were associated with electrons accelerated in solar flares or coronal flare-like events.

Introduction

Precipitating electrons that fill the magnetospheric polar cap poleward of the auroral oval have been reported by many investigators [e. g., *Winningham and Heikkila*, 1974; *Fairfield and Scudder*, 1985]. Termed "polar rain" by *Winningham and Heikkila* [1974], these electrons typically have energies of a few hundred eV with fluxes ~0.05 ergs cm^{-2} s^{-1} sr^{-1} [*Sotirelis et al.*, 1997]. They precipitate with a roughly uniform spatial distribution over one or the other polar cap. Polar rain has been attributed to anisotropic (aligned with **B**) suprathermal (halo) solar wind electrons [*Fairfield and Scudder*, 1985] that have direct access to that polar cap along open field lines [*Winningham and Heikkila*, 1974] in the same way that energetic solar-flare electrons do. *Fairfield and Scudder* [1985] called it the solar wind "strahl" and attributed its relatively high characteristic energy to a relative lack of collisional scattering by interplanetary electrons. *Foster and Burrows* [1976; 1977] reported observations of high-energy electrons in the polar cap with energy spectra peaked at ~100 eV and ~2 keV during periods of large-scale bow-shock expansion. Similar fluxes in the interplanetary medium and the dayside magnetosheath were not found while the fluxes above 1 keV were similar to those observed in the morningside plasma sheet. Thus the authors suggested that the electrons above 1 keV were accelerated by a potential barrier at the bow shock or within the magnetospheric cavity on field lines that intersected the distended bow shock.

Because of the unusually low solar wind densities (~0.1 cm^{-3}) immediately upstream from the Earth's bow shock attained on 11 May 1999, the magnetosphere must have had roughly twice its usual radius, and either polar cap must have had roughly half its usual area. The northern polar cap showed a roughly uniform illumination by precipitating electrons (energetic enough to produce 2–12 keV x-rays) during much of this time, while the southern polar cap was mostly "dark." This observation was revealed by a combination of measurements from the Polar Ionospheric X-ray Imaging Experiment (PIXIE) on NASA's GGS/Polar satellite and the particle detectors on four Defense Meteorological Satellite Program (DMSP) spacecraft. These measurements were combined with measurements of energetic electrons and radio waves by NASA's GGS/WIND spacecraft to reveal the solar origin of the electrons that produced the polar-cap x-rays.

PIXIE Measurements

PIXIE is a "multiple-pinhole" camera designed to image auroral bremsstrahlung x-rays produced by energetic electrons precipitating into the upper atmosphere. It is onboard NASA's Polar spacecraft, which follows a highly elliptical orbit with apogee at 8 R_E altitude and perigee at 0.8 R_E altitude. The present work is based on PIXIE measurements of ~2 – 12 keV x-rays; the efficiency of producing x-rays detectable by PIXIE increases rapidly with increasing electron energy >2 keV. (For a complete description of the instruments on the Polar and WIND spacecraft, see the special issues *Space Science Reviews, Vol. 71*, Nos. 1 – 4, 1995.)

PIXIE provided images from 1000 to 2000 UT on May 11, 1999 while operating on an 80% duty cycle (12 min on, 3 min off). Measurements from the ACE L1 spacecraft show that the solar wind density remained below 0.5 cm^{-3} throughout this time interval and reached a minimum of ~0.1 cm^{-3} near 1730 UT while the solar wind speed stayed around 350 – 400 km/s. The IMF (in GSM coordinates) remained rather steady with B_x ranging between –4 and –6 nT, B_y ranging between 2 and 5 nT, and B_z ranging between -1 and 3 nT. The top panels in Figure 1 show two PIXIE x-ray images selected from the observation period. Storm time PIXIE images typically show x-ray emissions extending equatorward from around the rim of the polar cap but with a notable minimum in the afternoon quadrant and require 2 – 5 min exposures to produce good x-ray images [see *Anderson et al.*, 2000] as opposed to the ~11.5 minutes required here. The x-ray emissions in Figure 1 instead fill a region above about 75° – 80° magnetic latitude (MLAT), with the emitting region centered a few degrees toward mid-morning (~0900 MLT) from the magnetic pole. Patches of enhanced x-ray flux in these images are about the size of PIXIE's spatial resolution ("pinhole" size) at apogee, and may well be smaller than they appear.

[1]Space Science Applications Laboratory, The Aerospace Corporation, El Segundo, CA.
[2]Space Physics Department, Lockheed Martin Advanced Technology Center, Palo Alto, CA.
[3]Space Sciences Laboratory, University of California, Berkeley.

Paper number 2000GL011983.
0094-8276/00/2000GL011983$05.00

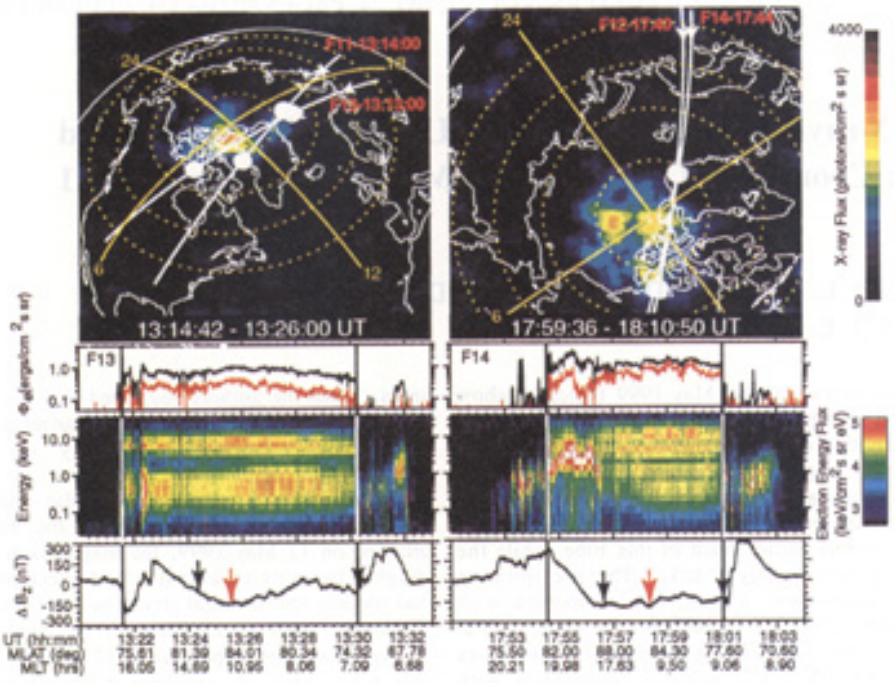

Figure 1. Two x-ray images selected from the PIXIE observation interval on 11 May 1999 (top panels) along with coincident DMSP measurements: the integrated electron energy flux (second row), electron energy flux (third row), and horizontal component of the magnetic field perturbations (bottom panels). The orbit tracks of DMSP satellites in the PIXIE field of view at these times, projected along **B** to 100 km altitude, are plotted on the images with the time at the start of the track indicated. White circles mark the spacecraft locations at the times indicated by the vertical lines in the color spectrograms. Red arrows in the bottom panels mark spacecraft traversal of the noon meridian, and black arrows span regions of decidedly open field lines.

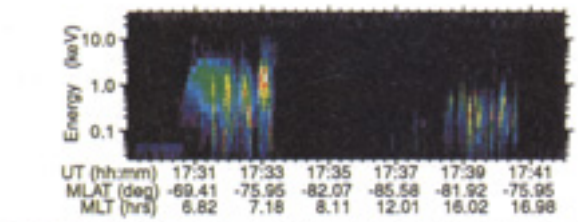

Figure 2. The DMSP precipitating electron data from a southern auroral pass near the time of the data in the right-hand column of Figure 1.

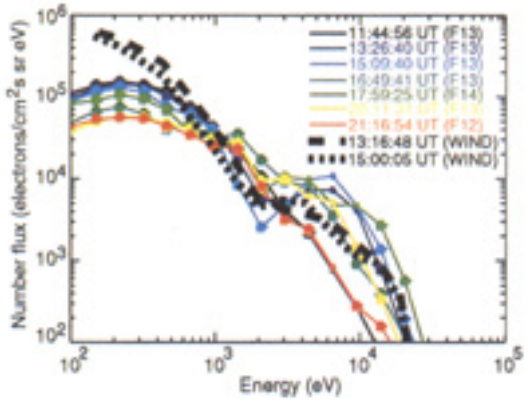

Figure 3. Seven DMSP electron number flux spectra accumulated over the regions identified as polar cap and two spectra measured by the WIND spacecraft.

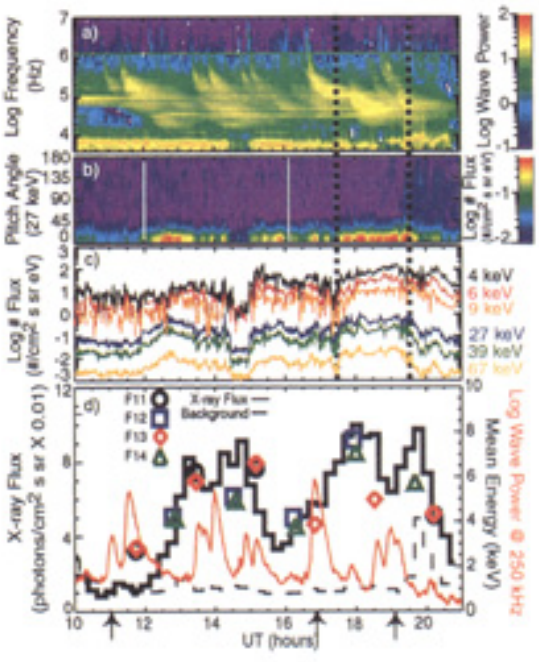

Figure 4. WIND measurements of (a) radio wave power, (b) pitch angle distribution of 27 keV electron number fluxes, and (c) electron number fluxes at various energies. (d) Total flux of x-rays emitted from geomagnetic latitudes >80° (solid black histogram), the level of the detector background (dashed black histogram), the mean electron energy above 1 keV (colored symbols) measured by SSJ4 within the regions identified as the polar cap, and the radio wave power at 250 kHz.

DMSP Measurements

The four DMSP spacecraft used in this study (F11 – F14) fly in Sun-synchronous orbits at altitudes ~840 km with ascending nodes at about 1800 solar local time (SLT) (F13), 1930 SLT (F11) and 2100 SLT (F12 and F14). They have orbital periods of ~101 min. The onboard instrument of primary interest here is the precipitating energetic particle spectrometer (SSJ/4) described by *Hardy et al.* [1984]. The SSJ/4 instruments measure electrons and ions in 20 energy channels ranging from ~32 eV to 32 keV at a sweep rate of once per second. The sensors are oriented so that their look direction is within a few degrees of local vertical, so they always look into the loss cone at high latitudes. The black traces in the second row of Figure 1 show the integrated precipitating electron energy flux measured along the paths of the F13 and F14 satellite tracks shown in the images. The red traces show the integrated energy flux weighted by the atmospheric x-ray production and instrument response functions (see *Anderson et al.* [2000] for a detailed discussion). Panels in the third row show DMSP SSJ/4 color spectrograms of precipitating electron energy flux. The particle data show significant electron precipitation up to 20 keV throughout the regions between the vertical solid lines. Electron precipitation appears in two bands (seen most clearly in the left spectrogram), one centered at a few hundred eV and the other centered at about 7 keV. Some part of these regions would normally be associated with the polar cap. Intensities in both the high- and low-energy components are greater on the morning side (the red arrows indicate the noon meridian) than on the evening side as also evidenced by the shift in the x-ray emissions toward ~0900 MLT. This is consistent with observations of a dusk-to-dawn asymmetry associated a positive IMF B_y [*Meng and Kroehl,* 1977] and a nightside-to-dayside intensity gradient in polar rain [e. g., *Gussenhoven et al.*, 1990]. Except on the nightside of the right-hand spectrogram, the spectral shape of the electron distributions changes little across the polar-cap region, as can be seen from the fairly constant ratio between the black and red traces in the integrated electron flux plots. The "inverted-V" auroral electron fluxes seen around 1755 UT at calculated magnetic latitudes >80° on the dusk side in Figure 1 would have produced little in the way of x-ray fluxes to be observed by PIXIE because their energies were too low.

The bottom panels in Figure 1 show the traces of ΔB_z, as measured by the DMSP onboard triaxial fluxgate magnetometers [*Rich et al.*, 1985]. These measurements help identify locations of Region-1 Birkeland currents that should characterize the polar-cap boundary. The data indicate the presence of field-aligned current (FAC) structures on either side of the pole. The dawnside FACs are associated with structured electron precipitation and weak high-energy ion precipitation (not shown here). However, the duskside FACs extend to >85° MLAT and exist largely within the region of diffuse electron precipitation that extends across the pole and within a region of cusp/mantle-like ion precipitation with latitudinally decreasing energy dispersion. On the basis of the DMSP measurements, we believe the spacecraft were on open field lines at least between the times indicated by black arrows in the bottom panels of Figure 1. This was verified with measurements of the high energy electrons (>500 keV) by NASA's low-Earth-orbiting SAMPEX spacecraft (not shown here) showing the location of the trapping boundary, believed to be a low-latitude limit for the last closed field line.

Figure 2 shows the SSJ/4 data from a southern auroral pass just prior to the time of the data in the right-hand column of Figure 1. The measurements are more typical of quiet time with an empty polar cap and weak precipitation on either side. The southern polar cap was empty throughout this time interval. Indeed interplanetary electrons should have had preferential access via reconnection to the northern polar cap during the entire period, since IMF B_x was negative the whole time [*Fairfield and Scudder*, 1985].

Electron number-flux spectra obtained from the regions bounded by the arrows in Figure 1, as well as from 5 other passes about evenly spaced in time between about 1130 and 2130 UT, are shown in Figure 3. These spectra show a low energy component with a broad peak around 200 eV, as is characteristic of polar rain. This component was seen continuously throughout the day but with a monotonically decreasing flux level. A second peak at about 7 keV is very pronounced in the passes at 1326 and 1509 UT. The secondary peak appears near 3.5 keV at 1649 and 1759 UT. A third "peak" appears near 9 keV at 1759 UT when the most intense x-ray fluxes of the day were observed. These changes in spectral shape are important because the efficiency at producing the 2 – 12 keV x-rays detectable by PIXIE increases very rapidly with electron energy >2 keV. The required electrons are much more energetic than the usual (~50 eV) tail of the solar-wind electron distribution and even more energetic than the 200 – 300 eV electrons that typically populate the solar corona. By 2100 UT, any secondary high energy component had completely disappeared leaving only the diminished typical "polar rain" component. The spectra indicated by the dashed lines were measured in the solar wind and will be discussed in the next section.

Further Measurements

Figure 4a shows a spectrogram of the radio waves measured by the WAVES experiment on board the WIND spacecraft during the time that PIXIE was observing the northern polar cap. WIND was ~50 R_E upstream of the Earth during this period; it encountered the bow shock at ~1730 UT and was in the magnetosheath during the period bounded by the vertical dashed lines in Figures 4a-c. Numerous radio bursts drifting down to near the local plasma frequency (indicated by the intense band of emissions in the 5 – 10 kHz range corresponding to local plasma densities of 0.3 – 1.24 cm^{-3}) were observed during this period. These type III radio bursts are produced by escaping solar electrons at energies from ~1 to 100 keV accelerated in flare or coronal flare-like events (see review by *Lin* [1990]).

Figure 4b shows the pitch angle distribution of the 27 keV differential electron number flux measured by the 3-D Plasma and Energetic Particle experiment (3-DP) on WIND, which provides measurements of electrons from ~10 eV to 300 keV. The data above 20 keV had a much larger signal-to-noise ratio than the data below 20 keV, thus the 27 keV data is plotted here. Prior to ~0700 UT, the distribution was isotropic but became very field aligned after 0700 UT and remained so throughout this time period as shown in Figure 4b. This was during the period of lowest solar wind density (<0.5 cm^{-3} - see Figure 4a) when the strahl was the strongest.

The field-aligned number fluxes measured by the 3-DP at selected energies are shown in Figure 4c. The fluxes began to increase after the first radio bursts near 1100 and 1130 UT. After that, the fluxes were extremely variable with a flux dropout near 1430 UT. The two 3-DP spectra shown in Figure 3 (multiplied by 50) are 9-min averages acquired ~10 minutes prior to two of the DMSP measurements, the approximate solar wind convection time from WIND to the Earth. They both show a bump in the distribution between 3 and 10 keV, similar to the DMSP measurements. Such double-peaked distributions were measured by 3-DP throughout much of the observation period. The magnitudes of the electron fluxes at WIND and DMSP differ by a factor of more than 50 because the strahl at WIND was <3.5° wide, and probably <1° wide [*Ogilvie et al.*, 2000] and filled less than 33% of the 3-DP acceptance angle of 22° (11° pitch angle) while the strahl at DMSP completely filled the SSJ4 45° acceptance angle.

PIXIE measurements of the rate of x-rays emitted from geomagnetic latitudes >80° are displayed as the solid black histogram in the bottom panel of Figure 4d with the dashed histogram indicating the level of detector background. The colored symbols represent the mean electron energy above 1 keV in the spectra measured by the DMSP spacecraft within the region identified as the "polar cap" (between the pairs of black arrows) as described in Figure 1. Note that the electron energy of peak production of atmospheric brehmsstrahlung x-rays collected by PIXIE for the measured DMSP spectra is on the order of 10 keV and most of the collected x-rays were produced by electrons with energies >10 keV. F11 and F13 crossed the polar cap almost simultaneously and although their orbits cut through different portions of the polar cap because their orbital planes differ in local time, the derived mean energies are nearly identical where available throughout the time period. This result indicates that the energy distribution of the precipitating electrons was spatially uniform.

The red line in Figure 4d indicates the radiowave power at 250 kHz measured by WAVE showing the approximate time of the type III radio bursts. The times of three solar x-ray flares reported by the GOES 8 satellite are indicated by arrows at the bottom of Figure 4. Only one of the flare locations (the second one) was near the west limb of the Sun and could thus be the source of the electrons seen at WIND. The first radio burst, associated with the first flare, did not result in any significant electron flux increase at WIND, as expected. The second radio burst was associated with a sudden jump in the fluxes at 27 keV about 25 minutes later, the approximate travel time of 27 keV electrons along the Parker spiral from the Sun to WIND, followed by delayed increases at lower energies, consistent with their travel times from the Sun. The x-ray emissions began to increase shortly after the sudden jump in the fluxes at 27 keV and peaked shortly after the 27 keV flux peaked. There was another sudden increase in the fluxes at 27 keV about 25 minutes after the fourth radio burst followed by a peak in the x-ray fluxes and a subsequent dropout in the electron and x-ray fluxes. The relationship between the electron fluxes measured at WIND and the polar-cap x-ray fluxes becomes more complex after this due to the nearly continuous acceleration of solar wind electrons indicated by the multiple radio bursts and the complications of magnetic conjugacy between WIND and the earth's polar caps. The electrons associated with type III radio bursts are often relatively narrow beams such that there is a strong gradient in electron flux across magnetic flux tubes. Thus, WIND and the polar cap must be on the same flux tube for direct comparison of electron and x-ray fluxes, a rare occurrence.

Conclusions

In summary, there was a strong hemispherical asymmetry in polar-cap electron precipitation on 11 May 1999 with significant energetic electron fluxes observed inside the northern polar cap but no comparable precipitation inside the southern polar cap. X-rays imaged by PIXIE filled the northern polar cap (>75° – 80°) during much of this time. The precipitating electron distributions contained at least two spectral components, one with a non-varying characteristic energy of ~200 eV, typical of polar rain although significantly more intense than usual, plus a second and possibly a third temporally varying spectral peak at energies ~3.5 – 10 keV. Both spectral components showed similar spatial structure consistent with previous polar rain observations for conditions of positive B_y. The lower-energy component showed a steady decrease in flux intensity with time but little change in spectral shape. The higher energy component showed considerable variability in differential number flux and spectral shape. This variability was consistent with the highly variable polar cap x-ray emissions. The electron fluxes measured at WIND showed sudden increases associated with type III radio bursts, subject to the transit time from the Sun for the measured energies. These increases were initially well correlated with the x-ray emissions, but the correlation was weaker later in the observation period due to the nearly continuous acceleration of solar wind electrons indicated by the multiple radio bursts and the complications of magnetic conjugacy between WIND and the earth's polar caps. The solar wind energetic electron distributions show multi-component spectra throughout most of the observation period similar to those measured in the polar cap.

Our interpretation is that the northern polar cap was connected to interplanetary magnetic field lines, thus providing interplanetary electrons preferential access. The lower-energy component of the polar-cap electron spectrum probably came from the suprathermal (halo) portion of the solar wind electron distribution. The higher-energy components were associated with electrons accelerated in solar flares or coronal flare-like events.

Acknowledgments. The work at Aerospace was supported by NASA Contract NAS5-30369 and NASA Grant NAG5-7938 and by the USAF under contract F04701-88-C-0089. The work at Lockheed Martin was supported by NASA Contract NAS5-30372. The work by D. Larson was supported by NASA grant NAG5-6928. The authors thank the WIND/WAVES team for the WAVES data. The DMSP data was provided by the Air Force Weather Agency and the GOES x-ray flare times were acquired from NOAA/SEC.

References

Anderson, P. C., et al., Global storm time auroral X–ray morphology and timing and comparison with UV measurements, *J. Geophys. Res.*, *105*, 15,757, 2000.

Fairfield, D. H., and J. D. Scudder, Polar rain: Solar coronal electrons in the Earth's magnetosphere, *J. Geophys. Res.*, *90*, 4055, 1985.

Foster, J. C., and J. R. Burrows, Electron fluxes over the polar cap 1. Intense keV fluxes during poststorm quieting, *J. Geophys. Res.*, *81*, 6016, 1976.

Foster, J. C., and J. R. Burrows, Electron fluxes over the polar cap 2. Electron trapping and energization on open field lines, *J. Geophys. Res.*, *82*, 5165, 1977.

Gussenhoven, M. S., and D. Madden, Monitoring the polar rain over a solar cycle: A polar rain index, *J. Geophys. Res.*, *95*, 10399, 1990.

Hardy, D. A., et al., Precipitating electron and ion detectors (SSJ/4) on the block 5D/Flights 6-10 DMSP satellites: Calibration and data presentation, *Tech. Rep. AFGL-TR-84-0317*, Air Force Geophys. Lab., Hanscom Air Force Base, Mass., 1984.

Lin, R. P., Electron beams and Langmuir turbulence in type III radio bursts observed in the interplanetary medium, in *Basic Plasma Processes on the Sun*, edited by E. R. Priest and V. Krishan, 467, Kluwar Academic Publishers, Dordrecht, Netherlands, 1990.

Meng, C.-I., and H. W. Kroehl, Intense uniform precipitation of low-energy electrons over the polar cap, *J. Geophys. Res.*, *82*, 2305, 1977.

Ogilvie, et al., Electrons in the low density solar wind, *J. Geophys. Res*, in press, 2000.

Rich, F. J., et al., Enhanced ionosphere-magnetosphere data from the DMSP satellites, *EOS*, *66*, 513, 1985.

Sotirelis, T., et al., Polar rain as a diagnostic of recent dayside merging, *J. Geophys. Res.*, *102*, 7151, 1997.

Winningham, J. D., and W. J. Heikkila, Polar cap auroral electron fluxes observed with Isis 1, *J. Geophys. Res.*, *79*, 949, 1974.

P. C. Anderson and D. L. McKenzie, Space Science Applications Laboratory, The Aerospace Corporation, P.O. Box 92957 M2/260, Los Angeles, CA 90009. (e-mail: phillip.c.anderson@aero.org)

D. W. Datlowe, J. D. Hawley, S. M. Petrinec, and M. Schulz, Space Physics Department, Lockheed Martin Advanced Technology Center, 3251 Hanover St., Palo Alto, CA 94304.

D. E. Larson, Space Sciences Laboratory, University of California, Berkeley, CA 94720.

(Received July 5, 2000; revised October 11, 2000;
accepted October 30, 2000)